Prediction of the High Frequency Behavior in Degraded Coaxial Connector Based on Neural Network

Q. Li[1], W. Yi[2], and J. Gao[3]
[1] Institute of Automation, Chinese Academy of Sciences, Beijing, China
[2] Department of Materials Engineering, Auburn University, Auburn, AL, USA
[3] School of Electronic Engineering, Beijing University of Posts and Telecommunications, Beijing, China
Email: liqingya726@163.com; weiyi.@auburn.edu; gjc@bupt.edu.cn

***Abstract*—Accurate prediction of high frequency behavior for the degraded contact surface is of great significance for the reliability evaluation of the connector. A prediction algorithm of neural network is proposed to forecast the high frequency scattering parameters under different degradation levels. The degraded high frequency parameters are extracted according to the developed equivalent model. Simulations are conducted to predict the scattering parameters at the specific frequencies using the BP (back propagation) and Elman neural networks, and the prediction accuracy is further compared. Moreover, the scattering parameters at 3.1GHz to 3.5GHz are predicted for the two degradation levels, which provides the variations under higher frequency.**

***Index Terms*—Contact degradation, high frequency characteristics, neural network**

I. Introduction

With the rapid development of wireless and radio frequency technologies, higher requests for the coaxial connectors have been put forward. Of particular interest is reliability when the connectors are exposed to the atmospheric environment or operated in other severe surroundings, which degrade the contact surface by contamination or corrosion. Meanwhile, these effects would deteriorate the high frequency performances and decrease the reliability. Through investigation and analysis, the high frequency behaviors of connectors are closely related to more factors, such as surface microscopic features, structure, size, material, corrosion properties, and so on, which brings many difficulties, and the process of calculation the high frequency parameters is complicated. Fortunately, the development of artificial intelligence technology provides a new approach to predict the high frequency characteristics of degraded connectors, which ignores the details of the connector, so that the prediction of high frequency parameters becomes convenient.

Manuscript received August 12, 2021; revised September 23, 2021; accepted September 28, 2021.

Corresponding author: Q. Li (email: liqingya726@163.com).

This work was supported by the National Natural Science Foundation of China under Grant 51877010.

For the research of the degradation of contact interface, the effects of the impedance properties including resistance, capacitance, and inductance for connector's contact surface at high frequency were previously investigated [1]. Considering a typical multipoint contact interface, the high frequency effects of a degraded contact surface were estimated [2]. Angadi *et al*. [3] summarized the research about the finite element modeling of electrical connectors including the bulk regions and contact areas. The high frequency characteristics (return loss and insertion loss) were analyzed for coaxial connectors subjected to different corrosion levels [4]. Jin *et al*. [5], [6] analyzed the influences of contact pressure and environmental temperature on the passive intermodulation in electrical connectors. Zhang *et al*. [7] explored the electrical contact failure mechanism of connectors using the high-frequency contact impedance model. The variations of contact impedance were studied by finite-element simulations and experiment results.

The artificial neural network showed good performance in the analysis and prediction of complex characteristics. Xu *et al*. [8] developed a deep neural network model to predict the time-domain reflectometer impedance for differential vias in high-speed printed circuit boards. Song *et al*. [9] predicted the electromagnetic susceptibility of the Balise transmission module (BTM) system using a neural network method and the predicted data validated the measured results. Shu *et al*. [10] proposed an equivalent dipole model hybrid with the artificial neural network to evaluate electromagnetic interference (EMI), which would be helpful for the EMI diagnosis. Scharff *et al*. [11] predicted the S-parameters and figures of merit using artificial neural networks for the high-speed digital interconnects up to 100GHz. Therefore, the neural network method was adopted to predict the high frequency performance of degraded coaxial connectors, which is of substantial value to the reliability of connectors.

In the current paper, an artificial neural network technique for high frequency performance prediction of degraded coaxial connectors is presented. An equivalent model with the degraded contact interface was developed to simulate the connectors with different degradation

levels, and the degraded high frequency scattering parameters were extracted, which were then applied to the training data. Next, the scattering parameters data at 0.01MHz to 2.5GHz together with the BP and Elman neural networks were used to conduct the training and predict the scattering parameters at 2.6GHz, 2.7GHz, 2.8GHz, 2.9GHz, and 3.0GHz. Besides, the prediction accuracies of the two neural networks were compared. Finally, the high frequency scattering parameters at 3.1GHz to 3.5GHz were predicted using the Elman neural network.

II. Equivalent Model Developmemt

A. Sample Obtained

Fig. 1 shows the device under test (DUT), which contains a male to female coaxial connector and a female to female coaxial connector. The male to female coaxial connector was degraded after experiencing an accelerated corrosive environment. The scattering parameters of coaxial connectors with two degradation levels were measured using an Agilent network analyzer E5071C at frequencies from 0.01MHz to 3.0GHz. The connectors were corroded for 5 hours using the acid vapor with 65%-69% concentration to get the first and second degradation level samples.

Fig. 1. Device under test (DUT)

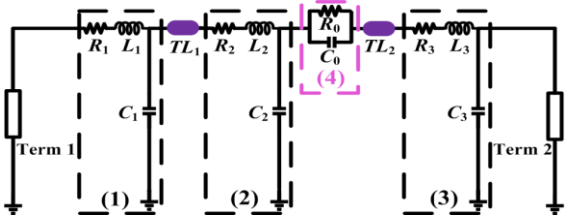

Fig. 2. Equivalent model of the DUT

B. Equivalent Model

In order to describe the high frequency characteristics of degraded coaxial connectors, an equivalent model is developed, as shown in Fig. 2. As depicted in Fig. 2, for the fresh samples, two types of the model including two transmission line models (TL_1 and TL_2 represent the male to female connector and female to female connector, respectively), and three contact models are established. The contact models are represented using part (1), part (2), and part (3), which describe the contact regions between the male side of the input cable and female side of the male to female connector, between the male side of the male to female connector and one side of the female to female connector, and between the other side of the female to female connector and the male side of the output cable, respectively. The three parts have an identical configuration, which is a series circuit consisting of a resistance (R_1, R_2, or R_3) and an inductance (L_1, L_2, or L_3), and then a shunt circuit composing of a capacitance (C_1, C_2, or C_3). The resistance and inductance are formed resulting from the contacts of each pin and receptacle, respectively. The capacitance is formed between the contact surface of the pin and receptacle. As the connectors are exposed in the corrosion environment, an additional contact element (4) containing a parallel circuit of resistance R_0 and capacitance C_0 appears in the equivalent model. Meanwhile, the other parts stay the same. The resistance increases with the degradation increases, while the capacitance decreases.

Based on the equivalent model of the DUT, the simulations can be conducted with two different degradation levels. Comparisons of experimental measurements and simulation results are shown in Fig. 3 (a) and Fig. 3 (b), which show good correlations. The solid and short dashed lines describe the experimental and simulation results, respectively. Because of the symmetry and reciprocity of the connector structure, S_{11}=S_{22}, S_{21}=S_{12}, and the S_{11} and S_{21} parameters can reflect the connector's behavior. Accordingly, the S_{12} and S_{22} parameter curves will not display in the following sections, and only the S_{11} and S_{21} parameters are adopted to analyze the characteristics.

Inspection of Fig. 3 (a) and Fig. 3 (b) shows that for the degradation level one (with a slight degree of degradation), the S_{11} and S_{21} parameters increase and decrease with the increase of frequency, respectively. Whereas for the degradation level two (with severe degradation), an opposite property can be observed for the S_{11} and S_{21} parameters, which decrease and increase as the increase of frequency, respectively. The values of resistance R_0 and capacitance C_0 are 0.001Ω and 15pF for the first and 12Ω and 7pF for the second degradation levels. The model parameter values in [12] are referenced for the fresh condition, whereas for the degraded condition, the model parameter values were determined using a data fitting technique in the simulation software.

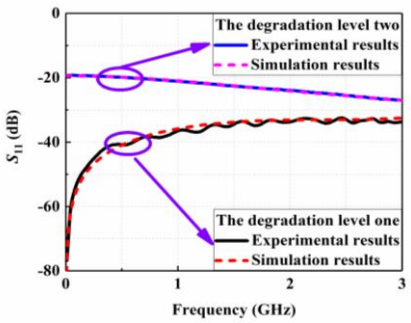

(a) S_{11} parameter

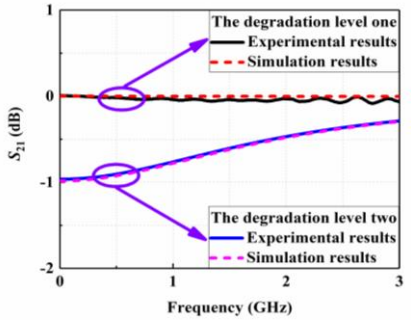

(b) S_{21} parameter

Fig. 3. High frequency behavior of experimental and simulation S parameter results for the first and second degraded connectors

However, the deterioration of connector is represented by R_0 and C_0 of the equivalent circuit model, which is confined to frequencies ranging from 0.01MHz to 3.0GHz due to its limited applicability. When the frequency is higher than 3.0GHz, the degraded model including the parallel of R_0 and C_0 is not suitable, whereas the influence factors such as skin effect, proximity effects are needed to be considered. Meanwhile, for the higher frequency, the effects of inherent nature such as structure, size, material for the connectors, and the characteristics of corrosion products on the high frequency performance become more sensitive. Accordingly, the degradation model becomes more sophisticated, and the high frequency behavior could not be characterized by the equivalent circuit model. Therefore, it is necessary to adopt the neural network for the prediction of high frequency characteristics based on the high frequency parameters at the lower frequencies, which is helpful to perfect the degradation behavior at all the frequency ranges.

III. Neural Network Model

As discussed previously, the high frequency characteristics will be affected by the increase in degradation. Due to the impedance properties of the degraded connectors, the S parameters will present different features at different frequencies. The next step is to develop an analysis methodology that will utilize this information to implement an effective method for predicting the high frequency performance. The approaches considered in this research are based on the BP and Elman neural networks. The details of the Elman neural network as an example are described in the following analysis.

The Elman neural network is a dynamic neural network with four layers including an input layer, a hidden layer, a context layer, and an output layer, as shown in Fig. 4. The structure of the Elman neural network is similar to the normal feedforward neural network. The context layer is used to record the previous outputs of the hidden layer and constitutes the interior feedback network combing with the hidden layer, which makes the Elman neural network a dynamic memory function. The nonlinear state expressions of the neural network are:

$$x(k) = f\left(W_1 x_c(k) + W_2 u(k-1)\right) \tag{1}$$

$$x_c(k) = a x_c(k-1) + x(k-1) \tag{2}$$

$$y(k) = g\left(W_3 x(k)\right) \tag{3}$$

where k is time, u is r dimension input vector, $x_c(k)$ is n dimension feedback state vector, $x(k)$ is n dimension element vector of hidden layer nodes, $y(k)$ is m dimension output node vector. W_1, W_2, W_3 have represented the connection weights from the content layer to the hidden layer, from the input layer to the hidden layer, from the hidden layer to the output layer, respectively. The coefficient a is defined as the self-connected feedback gain factor. $f(\ \ )$ and $g(\ \ )$ are represented the activation functions of the hidden layer neuron and output layer neuron, which are the sigmoid function $(1/(1+e^{-x}))$ and linear function, respectively.

E defined the loss function and can be expressed as:

$$E = \frac{1}{2}\left(y_d(k) - y(k)\right)^T \left(y_d(k) - y(k)\right). \tag{4}$$

where $y_d(k)$ is the actual output of step k for the network.

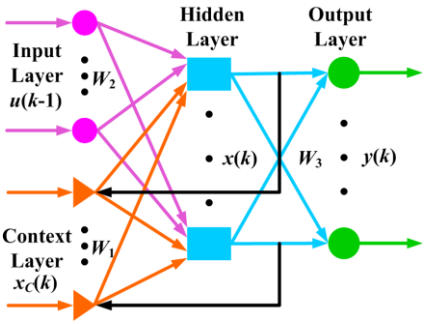

Fig. 4. Structure of the Elman neural network

TABLE I: Data for the Neural Network

Number	S_{11} (degradation level one)	S_{11} (degradation level two)	S_{21} (degradation level one)	S_{21} (degradation level two)
1	-67.6339	-19.4071	-0.00011	-0.9836
2	-54.6439	-19.4242	-0.00013	-0.98103
3	-48.6647	-19.4752	-0.00017	-0.97342
4	-45.2058	-19.5594	-0.00024	-0.961
5	-42.7937	-19.676	-0.00034	-0.94412
6	-40.9662	-19.8235	-0.00046	-0.92326
7	-39.5173	-20.0002	-0.0006	-0.89897
8	-38.3371	-20.2041	-0.00075	-0.87183
9	-37.3597	-20.433	-0.00091	-0.84247
10	-36.5424	-20.6842	-0.00108	-0.81147
11	-35.856	-20.9552	-0.00124	-0.77939
12	-35.2793	-21.243	-0.0014	-0.74674
13	-34.7964	-21.5448	-0.00155	-0.71398
14	-34.3948	-21.8576	-0.00169	-0.68147
15	-34.0644	-22.1784	-0.00182	-0.64953
16	-33.7967	-22.5042	-0.00192	-0.6184
17	-33.5843	-22.8323	-0.00201	-0.58829
18	-33.4202	-23.16	-0.00209	-0.55933
19	-33.2979	-23.4852	-0.00214	-0.53161
20	-33.2112	-23.8057	-0.00219	-0.50518
21	-33.1534	-24.1201	-0.00221	-0.48008
22	-33.1177	-24.4274	-0.00223	-0.45629
23	-33.0969	-24.7272	-0.00224	-0.43381
24	-33.0834	-25.0198	-0.00225	-0.41258
25	-33.0691	-25.3059	-0.00225	-0.39258
26	-33.0455	-25.5873	-0.00227	-0.37373
27	-33.004	-25.866	-0.00229	-0.35599
28	-32.9362	-26.1448	-0.00232	-0.33929
29	-32.8343	-26.4272	-0.00237	-0.32356
30	-32.6914	-26.7168	-0.00245	-0.30876
31	-32.5023	-27.0176	-0.00255	-0.29482

In contrast to the Elman neural network, there is no content layer in the BP neural network, and other layers have an identical structure with the Elman neural network. For the purpose of prediction, the S_{11} and S_{21} parameter values for the degradation level one and level two are used as training and testing data of BP and Elman neural networks. The values of resistance R_0 and capacitance C_0

of degraded conditions in the equivalent model are chosen ranging from 0.001Ω to 12Ω and from 7pF to 15pF, respectively. Accordingly, there are four columns data, including the S_{11} parameter curve for the first degradation degree, S_{21} parameter curve for the first degradation degree, S_{11} parameter curve for the second degradation degree, and S_{21} parameter curve for the second degradation degree. Each parameter curve contains 31 values, which were extracted as feature values ranging from 0.01MHz to 3.0GHz with an interval of 0.1 GHz, as shown in Table I. The frequency ranges of the training dataset and testing dataset were 0.01MHz to 2.5GHz and 2.6GHz to 3.0GHz, respectively. The values of S_{11} and S_{21} parameters are shown in Fig. 3 (a) and Fig. 3 (b) with the frequency ranging from 0.01MHz to 3.0GHz.

IV. Results and Discussion

According to the method in Section III, the S_{11} and S_{21} parameter values at the frequencies of 2.6GHz to 3.0GHz with an interval of 0.1GHz were predicted. The details were introduced with an example, and the prediction parameter values were located at 2.6GHz, corresponding to the 27th data in Table I. The data ranging from 1st to 26th are used to the training samples of the neural network, and the 27th data of S parameters are used to the testing samples. During the training process, every five values are as the inputs, and the sixth value is adopted to the output. Therefore, the network architecture had five input neurons, thirty hidden neurons, and one output neuron. Using the same method, the S_{11} and S_{21} parameter values at 2.7GHz, 2.8GHz, 2.9GHz, and 3.0GHz, corresponding to the 28th, 29th, 30th, and 31st values, can be predicted. The predicted and expected data were then compared to verify the accuracy of the neural network, mean squared error (MSE) was selected as a criterion. MSE can be expressed:

$$\mathrm{MSE}=\frac{1}{n}\sum_{i=1}^{n}\left[\left(f\left(x_i\right)-y(i)\right)\right]^2. \qquad (5)$$

where $f(x_i)$ is the testing data, $y(i)$ is the predicted data. n=100 is the number of samples. Based on the definition above, a lower MSE demonstrates better prediction accuracy. The training function trainlm and traingdx in the training process of neural network for the BP and Elman neural network, respectively. The maximum number of training epochs is 1000, the training error is 1×10^{-12}, the learning rate is 0.01, and the remaining training parameters are default values.

Fig. 5 (a) and Fig. 5 (b) depict the comparisons of expected and predicted data using the BP and Elman neural networks for the two degradation levels. Both of them have a small deviation between the prediction results and the actual data. The results indicate that the prediction results of the Elman neural network are closer to the expected data, and the MSE values are 0.56% and 0.53% for the BP and Elman neural networks, respectively. Accordingly, the Elman neural network reveals higher prediction accuracy. In the following analysis, the Elman neural network is selected to predict the S_{11} and S_{21} parameter values.

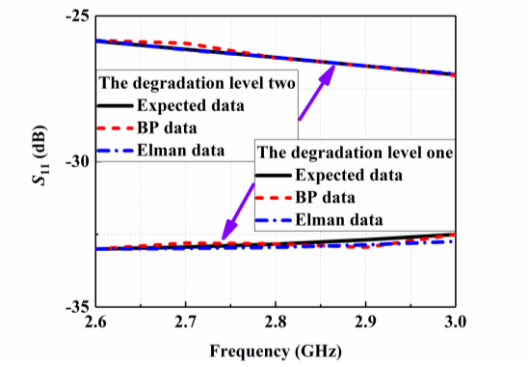

(a) S_{11} parameter

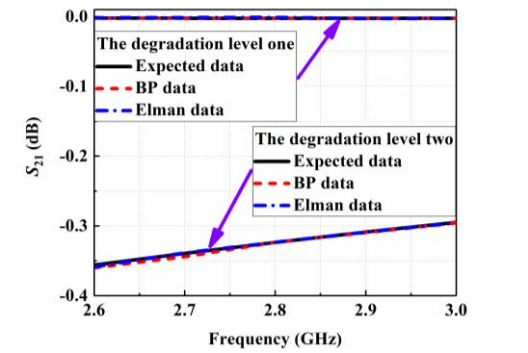

(b) S_{21} parameter

Fig. 5. The S parameter comparisons of expected and predicted data using the BP and Elman neural networks

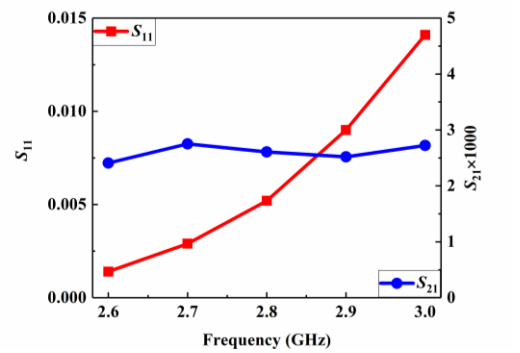

Fig. 6. MSE results

In the work, 100 simulations were carried out to generate the required samples. Then 100 MSE values were averaged in each frequency, and the MSE results of S_{11} and S_{21} parameters ranging from 2.6GHz to 3.0GHz are shown in Fig. 6. As depicted in Fig. 6, the MSE values of S_{11} parameters increase with the increase of frequency, which are lower than 0.015 within the research frequencies. MSE values of S_{21} parameters are approximately ranging from 2.5×10^{-3} to 2.8×10^{-3}, which are extremely small compared with the MSE of S_{11} parameters, which demonstrates a good prediction accuracy.

Based on the above analysis, it is found that Elman neural network can be used to predict the high frequency behavior of degraded connector samples. With this method, the S_{11} and S_{21} parameters would be predicted ranging from 3.1GHz to 3.5GHz with an interval of 0.1GHz under the degraded one and two levels, the results are shown in Fig. 7 (a) and Fig. 7 (b). The solid line and short dashed line are represented the original

results under the first and second degradation conditions at 1Hz to 3.0GHz. The data points with the rhombus shape are the test results, the circle and star shapes are the predicted results using the equivalent model and neural network method for first and second degradation cases at 3.1GHz to 3.5GHz, respectively. From these two pictures, it is concluded that the predicted results provide a more obvious vision to understand the variation of S_{11} and S_{21} parameters at a higher frequency.

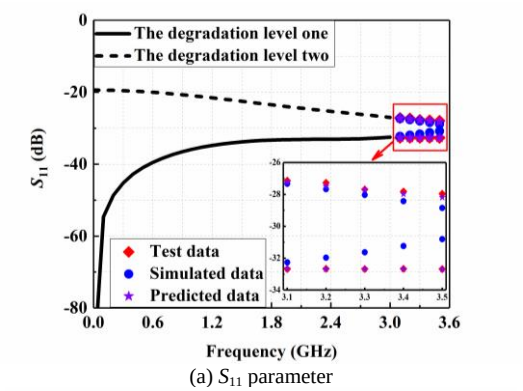

(a) S_{11} parameter

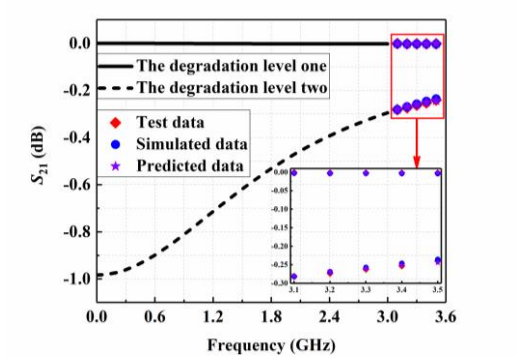

(b)S_{21} parameter

Fig. 7. The S parameter comparisons of expected and predicted data using the BP and Elman neural networks

V. Conclusion

In this work, an artificial neural network approach is employed to predict high frequency characteristics for degraded coaxial connectors. Firstly, an equivalent model with the degraded contact surface was developed. The scattering parameters at 0.01MHz to 3.0GHz under the first and second degradation levels were extracted, which were adopted as the training and testing data of BP and Elman neural networks. The S_{11} and S_{21} parameter values at 2.6/2.7/2.8/2.9/3.0 GHz were predicted using the two networks. The MSE values were 0.56% and 0.53% for the BP and Elman neural networks, respectively, which indicated that Elman neural network had a higher prediction accuracy. Besides, the S_{11} and S_{21} parameters ranging from 3.1GHz to 3.5GHz with the interval of 0.1GHz were predicted under the first and second degradation levels. The method applied in this research provides a possibility to predict the high frequency behavior at a higher frequency even terahertz.

Conflict of Interest

The authors declare no conflict of interest.

Author Contributions

Dr. Li conducted the research and wrote the paper; Mr. Yi provided guidance on structuring the paper and polished it; Prof. Gao provided review comments of the paper; all authors had approved the final version.

Acknowledgment

The authors wish to thank the Beijing Key Laboratory of Work Safety Intelligent Monitoring, Beijing University of Posts and Telecommunications, Auburn University, and Institute of Automation, Chinese Academy of Sciences. This work was supported in part by a grant from the National Natural Science Foundation of China.

References

[1] R. Timsit, "High speed electronic connectors: A review of electrical contact properties," *IEEE Trans. Electron.*, vol. E88-C, no. 8, pp. 1532-1545, Aug. 2005.

[2] R. Malucci, "High frequency considerations for multi-point contact interfaces," in *Proc. 47th IEEE Holm Conf. on Electrical Contacts*, Montreal, Quebec, Canada, 2001, pp. 175-185.

[3] S. V. Angadi, R. L. Jackson, V. Pujar, and M. R. Tushar, "A comprehensive review of the finite element modeling of electrical connectors including their contacts," *IEEE Trans. Compon. Packag. Technol.*, vol. 10, no. 5, pp. 836-844, May 2020,

[4] R. Ji, G. T. Flowers, J. Gao, Z. Cheng, and G. Xie, "High-frequency characterization and modeling of coaxial connectors with degraded contact surfaces," *IEEE Trans. Compon. Packag. Technol.*, vol. 8, no. 3, pp.447-455, March 2018.

[5] Q. Jin, J. Gao, L. Bi, and Y. Zhou, "The impact of contact pressure on passive intermodulation in coaxial connectors," *IEEE Microw. Wireless Compon. Lett.*, vol. 30, no. 2, pp. 177-180, Feb. 2020.

[6] Q. Jin, J. Gao, G. T. Flowers, Y. Wu, G. Xie, and L. Bi, "Effects of environmental temperature on passive intermodulation in electrical connectors," *IEEE Trans. Compon. Packag. Technol.*, vol. 10, no. 12, pp. 2008-2017, Dec. 2020.

[7] G. Zhang, L. Zhang, M. Li, X. He, L. Li, and M. Duan, "An evaluation method for electrical contact failure based on high-frequency impedance model," *IEEE Trans. Compon. Packag. Technol.*, vol. 11, no. 4, pp. 579-588, April 2021.

[8] J. Xu, J. Zhang, and J. Fan, "Application of deep learning for high-speed differential via TDR impedance fast prediction," in *Proc. IEEE Symp. Electromagnetic Compatibility, Signal Integrity and Power Integrity*, Long Beach, CA, 2000, pp. 645-649.

[9] Y. Song, Y. Wen, J. Zhang, Z. Cheng, and D. Zhang, "Fast prediction model for the susceptibility of balise transmission module system based on neural network," in *Proc. IEEE Symp. Electromagnetic in Advanced Applications*, Granada, Spain, 2019, pp. 445-448.

[10] Y. Shu, X. Wei, J. Fan, and T. Yang, "An equivalent dipole model hybrid with artificial neural network for electromagnetic interference prediction," *IEEE Trans. Microw. Theory Technol.*, vol. 67, no. 5, pp.1790-1797, May 2019.

[11] K. Scharff, C. M. Schierholz, C. Yang, and C. Schuster, "ANN performance for the prediction of high-speed digital interconnects over multiple PCBs," in *Proc. IEEE 29th Conference on Electrical Performance of Electronic Packaging and Systems (EPEPS)*, 2020, pp. 1-3.

[12] Q. Li, J. Gao, G. T. Flowers, Z. Cheng, G. Xie, and R. Ji. "Modeling and analysis of radio frequency connector degradation using time domain reflectometry technique," *Int. J. RF Microw. Comput. Aided Eng.*, vol. 30 no. 8, Aug. 2020.

Qingya Li received the B.E. degree from the College of Physics and Electronic Engineering, Shanxi University, Shanxi, China, in 2015, and the Ph.D. degree from the School of Electronic Engineering, Beijing University of Posts and Telecommunications, Beijing, China, in 2020. She is currently an assistant professor with the Institute of Automation, Chinese Academy of Science, Beijing, China. Her current research interests include electrical contact reliability, microwave device reliability, electromagnetic compatibility, and body channel communication.

Wei Yi received the B.S. degree from Hong Kong University of Science and Technology, Hong Kong, in 2012, and the M.S. degree from New York University, New York, NY, USA, in 2015. He is currently pursuing the Ph.D. degree in Materials Engineering at Auburn University, Auburn, AL, USA. His research interests include electronic materials, dielectrics and sensors.

Jinchun Gao received the B.S. and M.S. degrees from the Beijing University of Chemical Technology, Beijing, China, and the Ph.D. degree in electronic circuits and systems from the Beijing University of Posts and Telecommunications, Beijing. From 2009 to 2010, she was a visiting scholar with the Center for Advanced Vehicle and Extreme Environment Electronics, Auburn University, Auburn, AL, USA. She is currently a professor of electronic engineering with the Beijing University of Posts and Telecommunications. Her current research interests include electrical contact reliability and wireless communications.